Iron oxide inside SBA-15 modified with amino groups as reusable adsorbent for highly efficient removal of glyphosate from water

(Article begins on next page)

27 December 2024

Iron oxide inside SBA-15 modified with amino groups as reusable adsorbent for highly efficient removal of glyphosate from water

Sonia Fiorilli[a], Luca Rivoira[b], Giada Calì[b], Marta Appendini[b], Maria Concetta Bruzzoniti[b], Marco Coïsson[c], Barbara Onida[a]

[a] Dipartimento di Scienza Applicata e Tecnologia, Politecnico di Torino, Corso Duca degli Abruzzi 24, 10129 Torino, Italy

[b] Dipartimento di Chimica, Università degli Studi di Torino, Via P. Giuria 5, 10125, Torino, Italy
[c] INRIM, Electromagnetism Division, strada delle Cacce 91, I-10135 Torino, Italy

Abstract

Iron oxide clusters were incorporated into amino-functionalized SBA-15 in order to obtain a magnetically recoverable adsorbent. The physical-chemical properties of the material were characterized by FE-SEM, STEM, XRD, TGA, XPS, FT-IR and acid-base titration analysis.

Iron oxide nanoparticles were uniformly dispersed into the pore of mesoporous silica and that the adsorbent is characterized high specific surface area (177 m^2 /g) and accessible porosity.

The sorbent was successfully tested for the removal of glyphosate in real water matrices. Despite the significant content of inorganic ions, a quantitative removal of the contaminant was found. The complete regeneration of the sorbent after the adsorption process through diluted NaOH solution was also proved.

1.   Introduction

Human activities in several field is persistently connected to the disposal of a large number of various toxic pollutants. In recent years, water pollution has become a major issue, as a large amount of pollutants deriving from industrial and agricultural activities are found to cause serious adverse health effects on humans [1,2]. Wastewaters are contaminated by different sources, including plastic, textile, leather, cosmetics, paper-making, printing, and dye- manufacturing industries. In addition to those chemical pollutants, overuse of herbicides is another constant source of contamination of the environment, since herbicides give rise to toxicity and normally are persistent in soil [3–5]. In particular, glyphosate-based herbicides are currently among the most widely used agricultural chemicals globally. Glyphosate is a foliar absorption herbicide, which penetrates the cuticle by diffusion and it is rapidly transported throughout the plant tissue. In addition, sorption and degradation of glyphosate can be very different depending on soil composition,

however different studies showed that glyphosate is mainly adsorbed onto variable-charge surface sites (Al and Fe oxides) [6,7]. Therefore, long-term use of glyphosate, especially on oxide-poor soils, can lead to pollution of groundwater, in particular in areas with a shallow groundwater table.

In this context, there is a real need for powerful and reliable methods for the complete removal of herbicide from agricultural and domestic wastewaters and, as last stage, from drinking water.

Many of existing treatment technologies for decontamination, such as chemical coagulation or flocculation combined with flotation and filtration, membrane filtration, oxidation, and photo- degradation processes suffer from several drawbacks such as incomplete removal of pollutants, high-energy requirements, or production of toxic sludge and other waste products which need further treatment [8–10]. In the field of water remediation, adsorption process provides a highly versatile, eco-friendly and effective method to remove organic and inorganic contaminants. In addition, the possibility to regenerate the adsorbents and the relatively simple required procedures make adsorption a very convenient remediation strategy. For this aim activated carbon has been widely used because of its high adsorption capacity [11], however, the valuable costs of production and regeneration represent a significant drawback. Therefore, other classes of inorganic adsorbents with high surface areas have been used as alternatives to carbon-based adsorbents [12–16].

Among these mesoporous silicas, in the last decade, due to their high surface area, large and uniform pore size, and tunable pore structure have been tested as adsorptive removal of a wide range of contaminants [17–20]. Furthermore, the high exposed surface area can be easily functionalized with organic moieties, to impart specific hydrophilicity/ hydrophobicity or to introduce specific binding sites, with the aim to achieve very specific adsorbent − contaminants interactions [21] and thus high selective adsorption behaviour. Organically functionalized mesoporous silica have demonstrated their potential in application for removal of various organic contaminants, such as aromatic compounds, dyes, and pesticides [20]. For instance, SBA-15 modified with organic moieties, characterized by different hydrophobicity and acidity, has been successfully used as high capacity and selective sorbents for the removal of pharmaceuticals in water [22]. Large-pore mesoporous silica microspheres modified with alkyl chains (-C_{18}), tested for the extraction of phthalates, chosen as model hydrophobic compounds, in water samples, have shown very high capacity and fast adsorption kinetics [23]. Selective adsorption of negatively charged acid dyes in competitive adsorption studies involving various dyes has been conducted by charge-modified mesoporous silica through functionalization with ammonium groups [24]. Very recently, a new sorbent obtained by combining grafted amino groups and Fe (III) ions on SBA-15 surface has shown excellent adsorption behaviour towards tetracycline antibiotics from aqueous solution [25], confirming the ability of Fe ions to form stable complexes with organic molecules.

The adsorption capacity of iron-based adsorbents for removing contaminants (e.g. PO_4^{3-}, heavy metals, organic dyes) in different matrices (e.g., ground waters, surface waters, soils) has been extensively investigated in the literature [26–31]. Furthermore, magnetic iron oxide materials are useful for magnetic separation processes where an adsorbent can be separated from the solution using an applied magnetic field, which allows a convenient and low-cost strategy for the recovery of the adsorbents in a multiphase suspension without using extra organic solvents and additional filtration steps. Additionally, magnetically recovered adsorbents can be at a further stage regenerated by elution of

adsorbed contaminants, and, in specific cases, the re-elution in reduced volume of different solvents is essential for their extraction and enrichment in view of further analysis [24–32].

Therefore, the integration of functionalized mesoporous silica with iron oxide nanoparticles to obtain a magnetic nanocomposite characterized by enhanced adsorption behaviour, due to the combination of the adsorption properties of both of these materials, is undoubtedly an attractive remediation strategy. In order to attain this aim, in this work, a magnetic nanocomposite based on iron oxide nanocrystals included within the pores of an SBA- 15, modified with amino groups, has been prepared, characterized and tested in the adsorption of glyphosate from water samples. The optimal pH for the adsorption has been chosen, on the basis of the pK values of glyphosate (Scheme 1) and grafted amino groups, in order to enhance adsorption of glyphosate through the electrostatic interactions between the molecule functionalities and the surface binding sites. The regeneration of the material has been also investigated.

2. Experimental

Materials

All reagents used throughout this work were of analytical grade. Ordered mesoporous silica (SBA-15 type) were purchased from ACS Material (Advanced Chemical Supplier, USA). Iron (III) nitrate nonahydrate (98%), (3-aminopropyl) triethoxysilane (APTES, 99%), toluene (99.8%), ethanol and acetone (>99%), were purchased from Sigma Aldrich (Chemie, Steinheim, DE). Hydrochloric acid (35% w/w, d = 1187 g/ml) and NaOH (>98%) were from Carlo Erba (Milano, IT). Glyphosate and H2SO4 (95–97%, d=1.84g/ml) were from Sigma-Aldrich. High-purity water (18.2Mohm×cm resistivity at 25°C), produced by an Elix-Milli Q Academic system (Millipore, Vimodrone, MI, Italy) was used for standard and eluent preparation.

Samples preparation

The magnetic nanocomposite was obtained by means of the incipient wetness method. Specifically, 3 g of SBA-15 were impregnated with an aqueous solution of $Fe(NO_3)_3 * 9H_2O$ salt, which was obtained dissolving 3.2g of the salt in 5mL of bi-distilled water. After impregnation, the powder was dried in an oven at 80°C for 12 h. The impregnated SBA-15 was then annealed at 700 °C for 12 h in air (first oxidising thermal treatment) and at the same temperature for 12h in Ar+5% H_2 gas atmosphere (second reducing thermal treatment) [33]. The obtained sample is referred hereafter as RED-Fe-SBA-15.

For surface functionalisation RED-Fe-SBA-15 (1 g) was added to 200 mL of toluene and the obtained suspension was stirred at ambient temperature for 1 h, then the temperature was raised to 383 K and APTES (1% v/v) was added dropwise. The reaction was carried out at 383 K for 24 h, the powder was then recovered by filtration, washed three times by

toluene and dried at 353 K overnight. The obtained sample is referred hereafter as RED-Fe-NH$_2$-SBA-15.

Characterisation methods

X-ray diffraction (XRD) patterns were obtained using a PANalytical X'Pert Powder (Cu Kalpha radiation) diffractometer.

TG analyses were carried out between 298K and 1073K in air (flow rate 100 mL/min with a heating rate of 10 K/min) using a SETARAM 92 instrument and used to estimate the amount of grafted amino groups in RED-NH$_2$-Fe-SBA-15 sample. Specifically, RED-NH$_2$-Fe-SBA-15 and RED-Fe-SBA-15 (the reference sample) were first normalized against the dry weight, then the reference was subtracted from the RED-NH$_2$-Fe-SBA-15 sample, and the mass loss was normalized to the mass of the substrate to yield the mass increase (in wt%) from the amino functionalization step.

Nitrogen adsorption isotherms were measured using a Quantachrome AUTOSORB-1 instrument. Prior to nitrogen adsorption, samples were outgassed at 393 K for 5 h. BET specific surface areas were calculated in the relative pressure range 0.04–0.1 and the pore size distribution were determined through the DFT (Density Functional Theory) method, using the NLDFT equilibrium model for cylindrical pores.

Field Emission Scanning Microscopy (FESEM) and Scanning Transmission Electron Microscopy (STEM) images were recorded with a ZEISS MERLIN instrument, equipped with an EDS detector (Oxford Instruments).

A PHI 5000 Versaprobe II Scanning X-ray Photoelectron Spectrometer, equipped with a monochromatic Al K-alpha X-ray source (1486.6 eV energy, 15 kV voltage and 1 mA anode current), was used to investigate surface chemical composition. A spot size of 100 [?]m was used in order to collect the photoelectron signal for both the high resolution (HR) and the survey spectra. Different pass energy values were exploited: 187.85 eV for survey spectra and 23.5 eV for HR peaks. The core level spectra were deconvoluted with a nonlinear iterative least squares Gaussian fitting procedure.

For FTIR measurements powders were pressed in self- supporting wafers and spectra were recorded at room temperature with a Bruker Tensor 27 spectrometer operating at 2 cm^{-1} resolution, after outgassing the sample at 373 K for 1 h (residual pressure equal to 0.1 Pa).

Magnetic measurements were performed using a vibrating sample magnetometer (VSM), LakeShore model 7410. The measurement has been performed at room temperature under a maximum field of 17 kOe.

Titration of amino groups

In order to evaluate the dissociation constant of the amino groups bonded to the sorbent surface and sorbent capacity, titration measurements were performed according to the method proposed by Soldatov [34], using a EA-920 pH-meter (Orion Research Inc., Beverly, MA, USA) with an Ag/AgCl reference electrode.

Adsorption experiments

The performance of RED-Fe-NH_2 -SBA-15 sorbent in the removal of glyphosate was tested on a water sample collected after the potabilization process, which takes place in the Torino water treatment plant (IT).

These samples were characterized in terms of pH and conductivity measured at 20 °C (pH 7.4 and 490 μS/cm, respectively). The concentration of the main anions and cations (regulated by the Italian Legislative Decree 31/2001, on Drinking Waters) was also determined, in order to evaluate possible competitive interactions towards the sorbent surface. Concentrations of anions and cations were 13 mg/L Cl^-, 32 mg/L $NO3^-$, 35 mg/L $SO42^-$, 167 mg/L $HCO3^-$ and 1 mg/L K^+, 6 mg/L Na^+, 13 mg/L $Mg2^+$, 85 mg/L $Ca2^+$.

Batch adsorption experiments were performed on tap water samples, spiked with glyphosate standard to have a final glyphosate concentration of 2 mg/L in a volume of 17.5 mL. The tap water samples were put in contact with 0.1 g of sorbent. The pH of herbicide's solution was chosen according to the pK values of glyphosate (Scheme 1) and grafted amino groups (as determined by procedure described in Section 2.4).

The mixture was stirred in an orbital shaker for 24 h. The solution was then filtered through a mixed cellulose ester membrane (0.45 μm) and the filtrate was injected in an ion chromatographic system and analysed to determine glyphosate concentration, under optimized chromatographic conditions. For chromatographic separations, a 4000i chromatograph (Dionex, Thermo Scientific, Sunnyvale, CA, USA), equipped with IonPac AG16 (50 × 4 mm) guard and IonPac AG16 (250 × 4 mm) analytical column (Dionex, Thermo Scientific, Sunnyvale, CA, USA), with a 25 μL-injection loop and with a conductivity detector was used. The mobile phase was a 35mM sodium hydroxide solution. Detection was performed by chemical suppressed conductivity using a 50 mM H_2SO_4 regenerant solution and a AMMS III (4 mm) membrane suppressor obtained from Dionex Thermo Scientific. Eluent flow rate was set at 1.0 mL/min. Chromatographic data were collected and handled by PeakNet 2.8 software (Dionex, Thermo Scientific), without applying data correction or smoothing. The peak area obtained for glyphosate after injection of filtrate solution (Afiltrate) was compared with the one obtained by the injection of a tap water sample, spiked with 2 mg/L glyphosate, which was not put in contact with the sorbent (Astandard) in order to compensate for any matrix effect induced in glyphosate detection.

The percentage of glyphosate adsorbed%GLYadswas calculated according to the following equation:

%GLYads = (1 - Afiltrate / Astandard) * 100   [1]

Removal procedure was tested in triplicate.

3.   Results and Discussion

Structural and chemical characterisation of functionalised materials

RED-Fe-SBA-15 sample was characterized by STEM analysis, shown in Fig. 1(a–b), to investigate the size and dispersion of iron oxide. Reported images evidence that nanoparticles with a spheroidal shaped and size between 10 and 20 nm were effectively and homogenously confined inside the SBA-15 particles, without aggregation on the external surface. The mesoporous structure is still discernible in STEM micrographs after high-temperature reducing treatment and it will be further investigated by N_2 adsorption-desorption analysis. An EDS spectrum collected on RED-Fe-SBA-15 sample is shown in Fig. 1c. The elemental analysis identified the presence of Fe, which is attributed to the iron oxide nanocrystals embedded inside the silica support, with a concentration of 12.7% w/w, (obtained as average of 3 measurements): a value very close to the used iron nominal fraction corresponding to 14,7% w/w.

The wide-angle XRD patterns of SBA-15 and RED-NH_2-Fe-SBA- 15 supports are shown in Fig. 2a. The parent SBA-15 exhibits three well-resolved peaks at 0.93°, 1.60° and 1.85° 2theta, which respectively correspond to (1 0 0), (1 1 0), and (2 0 0) reflections of the hexagonally ordered porous structure, with a unit cell parameter of 11.0 nm, calculated as a0 = 2d100 /√3. The pattern of RED-NH_2 - Fe-SBA-15 shows reflections at slightly higher 2theta values, 0.99°, 1.71° and 1.97° , with a unit cell parameter of 10.3 nm, evidencing that the deposition of iron-oxide nanoclusters and the successive amino- functionalization do not change significantly the original hexagonal structure. The slight shrinkage of the unit cell parameter can be reasonably ascribed to a densification of silica walls induced by the two consecutive thermal treatments conducted at 973 K. The wide-angle XRD pattern of RED-NH_2-Fe-SBA-15 (Fig. 2b) evidences the presence of reflection peaks ascribable to differ- ent crystalline phases. Specifically, the broad band centred at 2theta = 22° can be assigned to the characteristic reflection from amorphous SiO_2 (JCPDS 29-0085) and the two peaks at 35.5° and 62.9° are ascribed to (311) and (440) reflections of spinel structure of maghemite phase (JCPDS 39–1346). These peaks could be in principle associated to magnetite (JCPDS 79-0416), as well, which makes challenging to distinguish the two iron oxides from XRD pattern. The other diffraction peaks are attributed to an iron (II) silicate ($Fe_2 SiO_4$) phase, which is reported to form under high temperature reducing treatment [35].

Fig. 3 reports the nitrogen sorption isotherms of SBA-15, RED- Fe-SBA-15 and RED-NH_2 -Fe-SBA-15 (the curves are shifted for sake of clarity): type IV isotherms with parallel adsorption-desorption branches typical for mesoporous materials are observed. As expected, the volume adsorbed and the relative pressure value at which the capillary condensation occurs is downward shifted after the encapsulation of iron oxide clusters inside SBA-15 channels, as consequence of the pore size reduction, and this trend is more pronounced after amino groups grafting. The specific surface area, mesopore diameter, as determined by the equilibrium NLDFT method based on nitrogen sorption data at 77 K, and porous volume are reported in Table 1. A significant reduction in specific surface area, total pore volume, and mesopore size is observed, as expected for a successful grafting.

Nevertheless, the final material is characterized by a relative high SSA (177m^2/g) and a pore diameter (4.8 nm) which appears acceptable for a fair diffusion kinetics.

FT-IR spectroscopy has been used to assess the presence of anchored amino groups on RED-NH$_2$-Fe-SBA-15. The spectra of SBA-15, RED-Fe-SBA-15 and RED-NH$_2$-Fe-SBA-15 outgassed at 373K are reported in Fig. 4a. FT-IR spectrum of SBA-15 shows sharp band at ca 3747cm^{-1}, due to isolated silanols and a broad envelope centred at 3500 cm^{-1}, ascribed to H-bonded hydroxyl groups. After encapsulation of iron oxide clusters, the most significant change observed is the reduction of the intensity for the band at 3500cm^{-1}. This depletion could be ascribed both to the high thermal treatment, which is expected to induce the condensation of adjacent silanols, and to the presence of iron oxide clusters which may react with SiOH groups producing iron silicate through the formation of Si-O-Fe. In order to elucidate further this point the spectrum of RED-Fe-SBA-15 has been also registered at low frequencies: the relative curve and band assignments are shown in Fig. 4b. The spectrum shows, among the others, the presence of a shoulder at around 943 cm^{-1} ascribable to the stretching mode of Si O Fe bonds [36–38]. Furthermore, in the 650–500 cm^{-1}, the bands due to the nu (FeO) modes, ascribable to the Fe O bonds in maghemite phase, are observed [39].

The FT-IR spectrum of RED-NH$_2$ -Fe-SBA-15 shows, in the region 3300–3000 cm^{-1}, the stretching modes of NH$_2$ species and, in the region 2950–2850cm^{-1}, intense bands due to CH$_2$ stretching modes of propyl chains of the functional groups. At lower wavenumbers, a band at 1595 cm^{-1} is observed, which is due to the NH2 bending mode, whereas the two shoulders at around 1650 cm^{-1} and 1520 cm^{-1} are assigned to the bending mode of protonated amines [40].

The band due to isolated silanols is not observed, whereas a broad absorption centred at about 3000 cm^{-1} (to which bands due to CH2 stretching modes are superimposed) is visible. Both evidence reveal the occurrence of H-bonding between surface silanols and anchored NH2 species. Moreover, part of isolated silanols can be consumed by the reaction with functionalizing silanes [41].

The molar total concentration of amino groups has been estimated on the basis of the weight loss measured by thermogravimetric analyses. TG curve (shown in Fig. 5) of RED-NH$_2$-Fe-SBA-15 shows small weight loss at temperature below 370 K (release of adsorbed water) and a more significant weight loss between 623 and 823K, ascribable to the decomposition of the aminopropyl groups. The curve related to TG analysis of RED-Fe-SBA-15 is reported for comparison and it has been used as reference for the estimation of the amount of amino groups: a small weigh loss in the 623–823 K range is also observed, likely due to the release of water formed by silanols condensation. The estimated amount of amino groups for RED-NH$_2$ -Fe-SBA-15 resulted to be 1.3 mmol/g.

XPS analysis of RED-NH$_2$-Fe-SBA-15 has been also carried to better elucidate the nature of grafted functionalities. The related deconvoluted N 1s (shown in Fig. 6) spectrum exhibits three components at 399.1 eV, 400.6 eV and 401.7 eV. On the basis of the literature [42], the peaks at lower BE (399.1 eV) and at higher BE (401.7 eV) are ascribed, respectively, to free amines (NH2) and to protonated amines (NH$_3^+$), whereas the remaining component is tentatively ascribed to amino groups perturbed by iron cations (both Fe(II) and Fe(III) species present in maghemite and magnetite phases) exposed at the surface of incorporated nanoclusters [22].

The magnetic properties of the samples were measured by vibrating sample magnetometry and plotted in Fig. 7. The room temperature hysteresis loop is characterized by a coercive field of approximately 150 Oe, which suggests the presence of particles that are still in the ferromagnetic state at room temperature. Conversely, the magnetisation does not saturate even at the maximum applied field (1.7 T), a behaviour which could arise from the presence of iron oxide nanoparticles, or of canted or antiferromagnetic states at their surface, that follow a linear dependence with the applied magnetic field.

The dissociation constant of amino groups, bonded to the sorbent surface, has been evaluated using the procedure proposed by Soldatov. [34], as already applied by the authors [43]. The acid- basic strength of sorbents exhibiting ion-exchange properties is influenced by the affinity of their functional groups towards H^+ and OH^- species. For this reason, the titration process is an ion- exchange reaction between the counter ion of titrant species (A^-) and the hydroxyl ions, associated to the protonated amino groups (R). Accordingly, the following equation could be written (Eq. (2)):

$$R + A^- + H_2O \leftrightarrow RH^+A^- + OH^- \qquad\qquad [2]$$
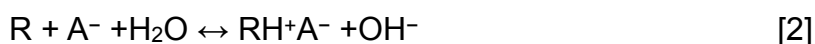
The titration of OH^- species displaced within the ion-exchange reaction has been performed by means of a 0.043 M standardized HCl solution.

As shown by Soldatov [34], the maximum of the first derivative of the titration curve (which represents the volume of titrating agent –HCl– added to reach the equivalent point) is equal to the number of active sites (NH3+) on the material surface (E, meq/g). The pK value could be easily extrapolated from the titration graph, since it corresponds to the value of pH where only half of the active sites are titrated (E/2).

The ion exchange capacity of the RED-NH_2-Fe-SBA-15 is 0.342 meq/g, a value significantly lower than the amount estimated by TG analysis. This incongruity is supposed resulting from two main reasons: the first is a most likely overestimation of amino groups obtained by thermogravimetric analysis, and the second is the presence, as evidenced by FT-IR and XPS data, of surface amino groups already protonated or interacting with Fe cations. The percentages of total area calculated for the deconvoluted spectrum of N1s (Fig. 6) are 48.7%, for the component at 399.1 eV, 24,5% for the component at 400.6 eV and 26,8% for the component at 401.7 eV. On the basis of these values more than half of amino moieties are not expected to be available for proton-transfer reaction and thus to be probed by titration.

The pK value obtained (7.6) is about 3 units lower than the bulk solution value (pK = 10.6 [44]), but still in agreement with the pK of APTES monolayer produced on silicon substrate and with the characteristic of surface amino groups [45].

The first derivative of the titration curve highlighted an additional maximum (pK 8.5) which was ascribed to the dissociation of Q2 silanols groups [46], as confirmed by titration of the SBA-15 support under the same procedure.

Removal of glyphosate from water solution

Results obtained by the characterization of RED-NH$_2$-Fe-SBA-15 evidenced textural and chemical features which strongly suggest the suitability of this sorbent for removal of glyphosate from water samples under proper experimental conditions. In fact, the exposed SSA, the average pore diameter and pore volume are large enough to promote fast diffusion kinetics of glyphosate inside the pore structure. In addition, adsorption interaction between glyphosate and RED-NH$_2$-Fe-SBA-15 is expected to take place both through the interaction with protonated amino groups and iron nanoclusters, via ion-exchange and chelation mechanisms [29], respectively, as recently demonstrated [47]. For the above mentioned reasons, the RED-NH$_2$-Fe-SBA-15 sorbent was tested for the removal of glyphosate from real samples matrices.

Since the presence of glyphosate in surface waters seems to be a relevant issue for drinking water processes, especially because its removal is greatly dependent upon the method employed during potabilization, [48], the removal properties of RED-NH$_2$-Fe-SBA-15 were tested on tap water samples, spiked with 2 mg/L of glyphosate. pH of water was adjusted to 2.1, in order to promote better ionic interactions between the positively charged protonated amino group of sorbent surface (pKa 7.6 for surface NH3 + species) and the negatively charged functionalities of herbicide. After 24 h of contact (equilibrium conditions reached, as experimentally verified), the solutions (filtered and analysed by ion chromatography) showed no more evidence of glyphosate (glyphosate concentration below the detection limit of the ion chromatographic method, 100 µg/L). Despite the significant content of inorganic ions in tap water, the sorbent exhibits quantitative removal, meaning that no competitive effects by ions of the matrix interfere with the adsorption of glyphosate onto the sorbent.

The development of sorbents to be used for purification of water matrices should not consider the adsorption of target molecules alone, but also the possibility to desorb them and reuse the material. For such reason, the same aliquots of RED-NH$_2$-Fe-SBA-15 previously tested in the removal studies, and thus containing adsorbed glyphosate, were tested for release. Under the assumption that ionic interactions between glyphosate and the amino groups of the sorbent play a crucial role in glyphosate adsorption, a 12.5 mM NaOH solution (pH 12.5) was used to release the herbicide. After 15 min of contact, the NaOH solution was filtered and analysed by ion chromatography, revealing that glyphosate retained on the sorbent surface was quantitatively released. Desorption of glyphosate was ascribed both to the reduced ion exchange capacity exhibited by RED-NH$_2$-Fe-SBA-15 at very basic pH (due to the deprotonation of amino groups, pK = 7.6) and to the competitive effect of the OH$^-$ counter ion in the ion exchange equilibrium. Chromatograms obtained for tap water sample analysed before and after the adsorption process, and for the solution of NaOH after the release treatment are shown and compared in Fig. 8.

Therefore, on the basis of the results obtained from both adsorption and desorption experiments, the synthesis of RED-NH$_2$-Fe-SBA-15 as sorbent for glyphosate removal seems justified by a quantitative retention of the herbicide and the subsequent complete regeneration of the material.

4.   Conclusions

A material based on iron oxide clusters incorporated into amino-functionalized SBA-15 was prepared in order to obtain a magnetically recoverable adsorbent with enhanced

adsorption behaviour. The physical-chemical properties were characterized by FE-SEM, STEM, XRD, TGA, XPS, FT-IR and acid-base titration analysis. The characterization results showed that iron oxide nanoparticles were uniformly dispersed into the pore of mesoporous silica and that the final material exhibits relatively high specific surface area ($177 \ m^2$ /g) and accessible porosity.

The obtained sorbent was successfully tested for the removal of glyphosate in real water matrices. Despite the significant content of inorganic ions, a quantitative removal of the contaminant was found, which strongly suggests the possibility of integration of this sorbent in wastewater treatment plants. The complete regeneration of the sorbent after the adsorption process through diluted NaOH solution was also proved.

References

[1] R.P. Schwarzenbach, B.I. Escher, K. Fenner, T.B. Hofstetter, C.A. Johnson, U. Von Gunten, B. Wehrli, The challenge of micropollutants in aquatic systems, Science 313 (2006) 1072–1077.

[2] J.M. Stellman, Encyclopaedia of Occupational Health and Safety, International Labour Organization, Geneva, Switzerland, 1998.

[3] R. Annett, H.R. Habibi, A. Hontela, Impact of glyphosate and glyphosate-based herbicides on the freshwater environment, J. Appl. Toxicol. 34 (2014) 458–479.

[4] N. Gilbert, A hard look at GM crops, Nature 497 (2013) 24.

[5] T.R. Roberts, J.S. Dyson, M.C. Lane, Deactivation of the biological activity of paraquat in the soil environment: a review of long-term environmental fate, J. Agric. Food Chem. 50 (2002) 3623–3631.

[6] O.K. Borggaard, A.L. Gimsing, Fate of glyphosate in soil and the possibility of leaching to ground and surface waters: a review, Pest Manag. Sci. 64 (2008) 441–456.

[7] I. Ololade, N. Oladoja, F. Oloye, F. Alomaja, D. Akerele, J. Iwaye, P. Aikpokpodion, Sorption of glyphosate on soil components: the roles of metal oxides and organic materials, Soil Sediment Contam.: Int. J. 23 (2014) 571–585.

[8] C. Adams, Y. Wang, K. Loftin, M. Meyer, Removal of antibiotics from surface and distilled water in conventional water treatment processes, J. Environ. Eng. 128 (2002) 253–260.

[9] S. Castiglioni, R. Bagnati, R. Fanelli, F. Pomati, D. Calamari, E. Zuccato, Removal of pharmaceuticals in sewage treatment plants in Italy, Environ. Sci. Technol. 40 (2006) 357–363.

[10] P.E. Stackelberg, E.T. Furlong, M.T. Meyer, S.D. Zaugg, A.K. Henderson, D.B. Reissman, Persistence of pharmaceutical compounds and other organic wastewater contaminants in a conventional drinking-water-treatment plant, Sci. Total Environ. 329 (2004) 99–113.

[11] L.C. Oliveira, R.V. Rios, J.D. Fabris, V. Garg, K. Sapag, R.M. Lago, Activated carbon/iron oxide magnetic composites for the adsorption of contaminants in water, Carbon 40 (2002) 2177–2183.

[12] B. Armagˇan, O. Özdemir, M. Turan, M. Celik, The removal of reactive azo dyes by natural and modified zeolites, J. Chem. Technol. Biotechnol. 78 (2003) 725–732.

[13] R.T.Carneiro,T.B.Taketa,R.J.G.Neto,J.L.Oliveira,E.V.Campos,M.A.deMoraes, C.M. da Silva, M.M. Beppu, L.F. Fraceto, Removal of glyphosate herbicide from water using biopolymer membranes, J. Environ. Manage. 151 (2015) 353–360.

[14] E.N. El Qada, S.J. Allen, G.M. Walker, Adsorption of methylene blue onto activated carbon produced from steam activated bituminous coal: a study of equilibrium adsorption isotherm, Chem. Eng. J. 124 (2006) 103–110.

[15] L.C. Oliveira, R.V. Rios, J.D. Fabris, K. Sapag, V.K. Garg, R.M. Lago, Clay–iron oxide magnetic composites for the adsorption of contaminants in water, Appl. Clay Sci. 22 (2003) 169–177.

[16] S. Wang, H. Li, S. Xie, S. Liu, L. Xu, Physical and chemical regeneration of zeolitic adsorbents for dye removal in wastewater treatment, Chemosphere 65 (2006) 82–87.

[17] D. Caldarola, D.P. Mitev, L. Marlin, E.P. Nesterenko, B. Paull, B. Onida, M.C. Bruzzoniti, R.M. De Carlo, C. Sarzanini, P.N. Nesterenko, Functionalisation of mesoporous silica gel with 2-[(phosphonomethyl)-amino] acetic acid functional groups. Characterisation and application, Appl. Surf. Sci. 288 (2014) 373–380.

[18] Y. Dong, B. Lu, S. Zang, J. Zhao, X. Wang, Q. Cai, Removal of methylene blue from coloured effluents by adsorption onto SBA-15, J. Chem. Technol. Biotechnol. 86 (2011) 616–619.

[19] L.-C. Juang, C.-C. Wang, C.-K. Lee, T.-C. Hsu, Dyes adsorption onto organoclay and MCM-41, J. Environ. Eng. Manage. 17 (2007) 29.

[20] A. Walcarius, L. Mercier, Mesoporous organosilica adsorbents: nanoengineered materials for removal of organic and inorganic pollutants, J. Mater. Chem. 20 (2010) 4478–4511.

[21] M.C. Bruzzoniti, R.M. De Carlo, S. Fiorilli, B. Onida, C. Sarzanini, Functionalized SBA-15 mesoporous silica in ion chromatography of alkali, alkaline earths, ammonium and transition metal ions, J. Chromatogr. A 1216 (2009) 5540–5547.

[22] T.X. Bui, S.-Y. Kang, S.-H. Lee, H. Choi, Organically functionalized mesoporous SBA-15 as sorbents for removal of selected pharmaceuticals from water, J. Hazard. Mater. 193 (2011) 156–163.

[23] Z. Li, D. Huang, C. Fu, B. Wei, W. Yu, C. Deng, X. Zhang, Preparation of magnetic core mesoporous shell microspheres with C18-modified interior pore-walls for fast extraction and analysis of phthalates in water samples, J. Chromatogr. A 1218 (2011) 6232–6239.

[24] Q. Qin, J. Ma, K. Liu, Adsorption of anionic dyes on ammonium-functionalized MCM-41, J. Hazard. Mater. 162 (2009) 133–139.

[25] Z. Zhang, H. Lan, H. Liu, J. Qu, Removal of tetracycline antibiotics from aqueous solution by amino-Fe (III) functionalized SBA15, Coll. Surf. A 471 (2015) 133–138.

[26] X. Chen, K.F. Lam, Q. Zhang, B. Pan, M. Arruebo, K.L. Yeung, Synthesis of highly selective magnetic mesoporous adsorbent, J. Phys. Chem. C 113 (2009) 9804–9813.

[27] R.A. Figueroa, A.A. MacKay, Sorption of oxytetracycline to iron oxides and iron oxide-rich soils, Environ. Sci. Technol. 39 (2005) 6664–6671.

[28] M. Iram, C. Guo, Y. Guan, A. Ishfaq, H. Liu, Adsorption and magnetic removal of neutral red dye from aqueous solution using Fe 3 O 4 hollow nanospheres, J. Hazard. Mater. 181 (2010) 1039–1050.

[29] L. Weng, W.H. Van Riemsdijk, T. Hiemstra, Factors controlling phosphate interaction with iron oxides, J. Environ. Qual. 41 (2012) 628–635.

[30] Y. Xu, L. Axe, Synthesis and characterization of iron oxide-coated silica and its effect on metal adsorption, J. Colloid Interface Sci. 282 (2005) 11–19.

[31] H. Zeng, B. Fisher, D.E. Giammar, Individual and competitive adsorption of arsenate and phosphate to a high-surface-area iron oxide-based sorbent, Environ. Sci. Technol. 42 (2007) 147–152.

[32] X.-S. Li, G.-T. Zhu, Y.-B. Luo, B.-F. Yuan, Y.-Q. Feng, Synthesis and applications of functionalized magnetic materials in sample preparation, TrAC Trends Anal. Chem. 45 (2013) 233–247.

[33] A. Parma, I. Freris, P. Riello, D. Cristofori, C. de Julián Fernández, V. Amendola, M. Meneghetti, A. Benedetti, Structural and magnetic properties of mesoporous SiO 2 nanoparticles impregnated with iron oxide or cobalt-iron oxide nanocrystals, J. Mater. Chem. 22 (2012) 19276–19288.

[34] V. Soldatov, A simple method for the determination of the acidity parameters of ion exchangers, React. Funct. Polym. 46 (2000) 55–58.

[35] N.-N. Wang, S.-Q. Zeng, X. Guan, Y. Wang, H.-F. Cheng, W.-Z. Wu, Preparation and characterization of magnetic iron nanoparticles encapsulated in mesoporous silica: the effects of reduction procedure and pore size, Mater. Lett. 112 (2013) 20–22.

[36] I.J. Bruce, T. Sen, Surface modification of magnetic nanoparticles with alkoxysilanes and their application in magnetic bioseparations, Langmuir 21 (2005) 7029–7035.

[37] P.I. Girginova, A.L. Daniel-da-Silva, C.B. Lopes, P. Figueira, M. Otero, V.S. Amaral, E. Pereira, T. Trindade, Silica coated magnetite particles for magnetic removal of Hg 2+ from water, J. Colloid Interface Sci. 345 (2010) 234–240.

[38] K.M. Khalil, A.A. Elsamahy, M.S. Elanany, Formation and characterization of high surface area thermally stabilized titania/silica composite materials via hydrolysis of titanium (IV) tetra-isopropoxide in sols of spherical silica particles, J. Colloid Interface Sci. 249 (2002) 359–365.

[39] S. Huang, P. Yang, Z. Cheng, C. Li, Y. Fan, D. Kong, J. Lin, Synthesis and characterization of magnetic FexOy@SBA-15 composites with different morphologies for controlled drug release and targeting, J. Phys. Chem. C 112 (2008) 7130–7137.

[40] A. Maria Chong, X. Zhao, Functionalization of SBA-15 with APTES and characterization of functionalized materials, J. Phys. Chem. B 107 (2003) 12650–12657.

[41] D. Brunel, A. Cauvel, F. Di Renzo, F. Fajula, B. Fubini, B. Onida, E. Garrone, Preferential grafting of alkoxysilane coupling agents on the hydrophobic portion of the surface of micelle-templated silica, New J. Chem. 24 (2000) 807–813.

[42] L. Zhang, J. Liu, J. Yang, Q. Yang, C. Li, Direct synthesis of highly ordered amine-functionalized mesoporous ethane-silicas, Microporous Mesoporous Mater. 109 (2008) 172–183.

[43] M.C. Bruzzoniti, A. Prelle, C. Sarzanini, B. Onida, S. Fiorilli, E. Garrone, Retention of heavy metal ions on SBA-15 mesoporous silica functionalised with carboxylic groups, J. Sep. Sci. 30 (2007) 2414–2420.

[44] R.C. Weast, M.J. Astle, W.H. Beyer, CRC Handbook of Chemistry and Physics, CRC press, Boca Raton, FL, 1988.

[45] H. Zhang, H.-X. He, J. Wang, T. Mu, Z.-F. Liu, Force titration of amino group-terminated self-assembled monolayers using chemical force microscopy, Appl. Phys. A: Mater. Sci. Process. 66 (1998) S269–S271.

[46] J.M. Rosenholm, T. Czuryszkiewicz, F. Kleitz, J.B. Rosenholm, M. Lindén, On the nature of the Brønsted acidic groups on native and functionalized

mesoporous siliceous SBA-15 as studied by benzylamine adsorption from

solution, Langmuir 23 (2007) 4315–4323.
[47] L. Rivoira, M. Appendini, S. Fiorilli, B. Onida, M. Del Bubba, M.C. Bruzzoniti,

Functionalized iron oxide/SBA-15 sorbent: investigation of adsorption performance towards glyphosate herbicide, Environ. Sci. Pollut. Res. 23 (2016) 21682–21691.

[48] J. Jönsson, R. Camm, T. Hall, Removal and degradation of glyphosate in water treatment: a review, J. Water Supply: Res. Technol.-AQUA 62 (2013) 395–408.

Scheme 1. Deprotonation reactions and relative pkaldpha values of glyphosate (www.chemicalize.org)

$pK_{a1} = 0.78$
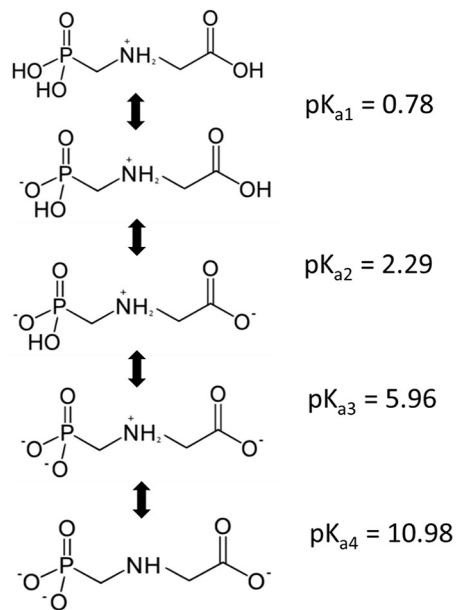
$pK_{a2} = 2.29$

$pK_{a3} = 5.96$

$pK_{a4} = 10.98$

Figure 1. (a) Bright field (BF) and (b) bright field + dark field (BF+DF) STEM images of RED-Fe-SBA-15. © Related EDS spectrum.
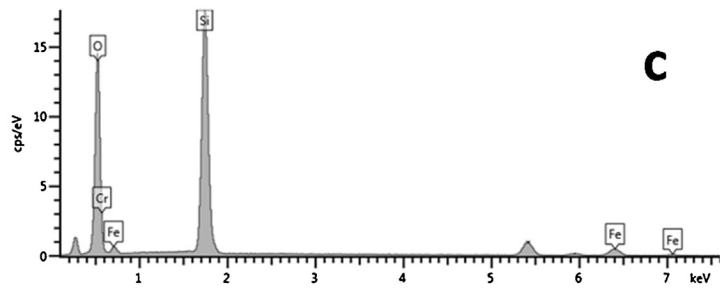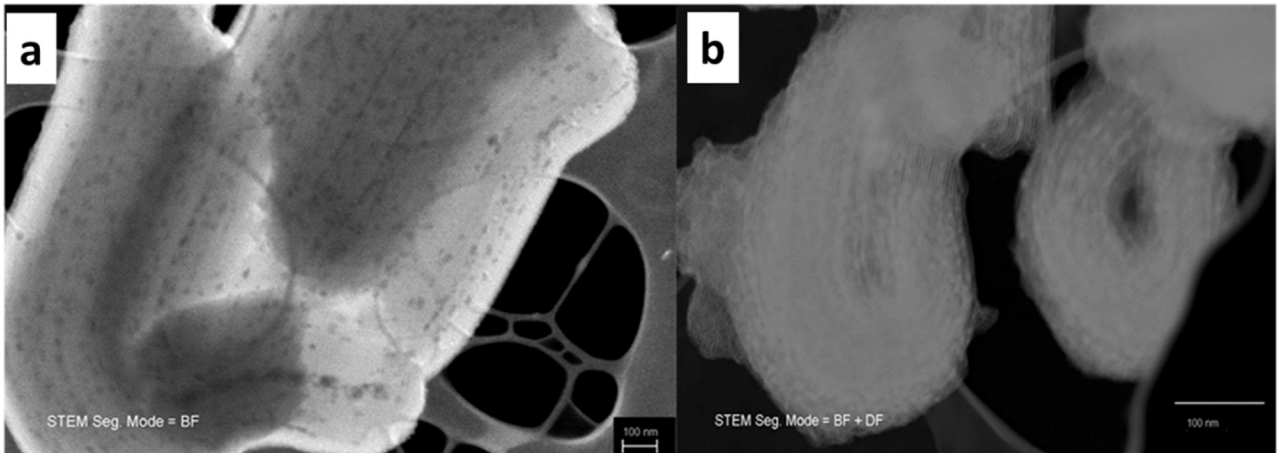
Figure 2. (a) Wide.angle XRD patterns of SBA-15 and RED-NH$_2$-Fe-SBA-15, (b) XRD pattern of RED-NH$_2$-Fe-SBA-15.
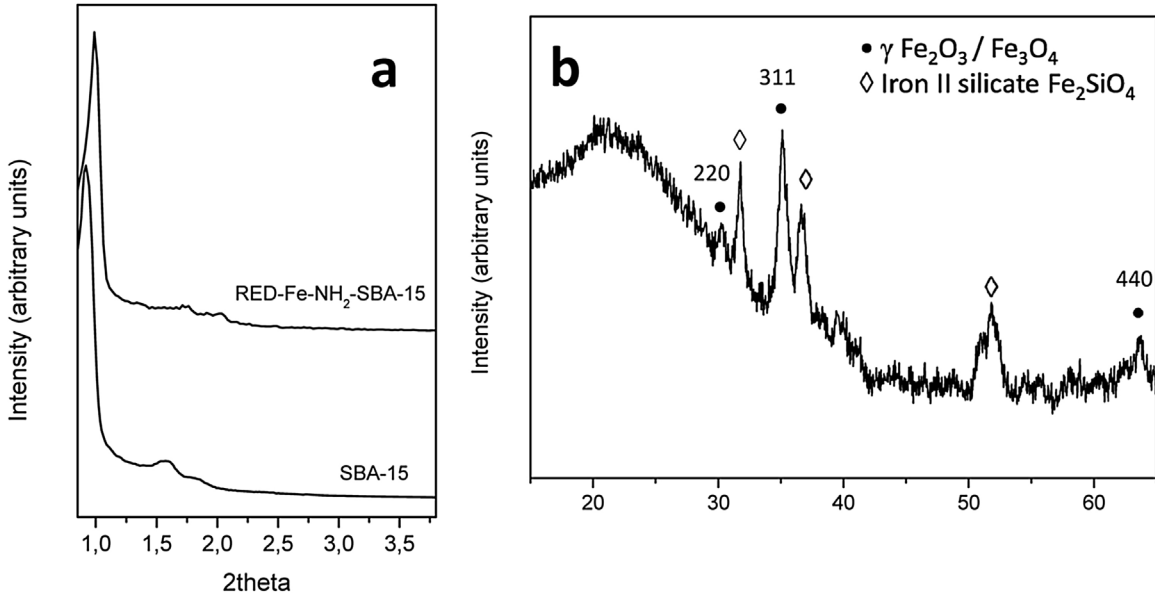
Figure 3. N$_2$ adsorption-desorption isotherms of SBA-15 (red), RED-Fe-SBA-15 (blue) and RED-NH$_2$-Fe-SBA-15 (black) and relative DFT pore size distributions.
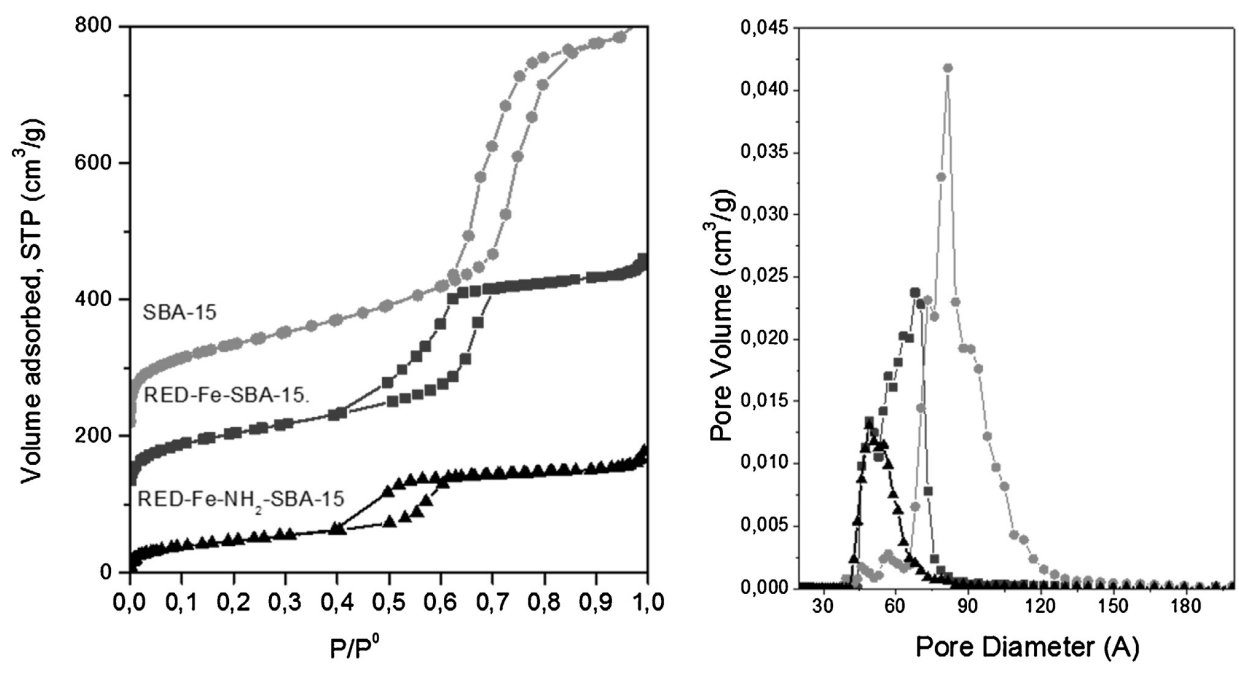
Figure 4. FT-IR spectra in 3800-1300 cm^{-1} range of SBA-15, RED-Fe-SBA-15 and RED-NH$_2$-Fe-SBA-15 (a) and FT-IR spectrum of RED-Fe-SBA-15 in 1200-400 cm^{-1} range (b).
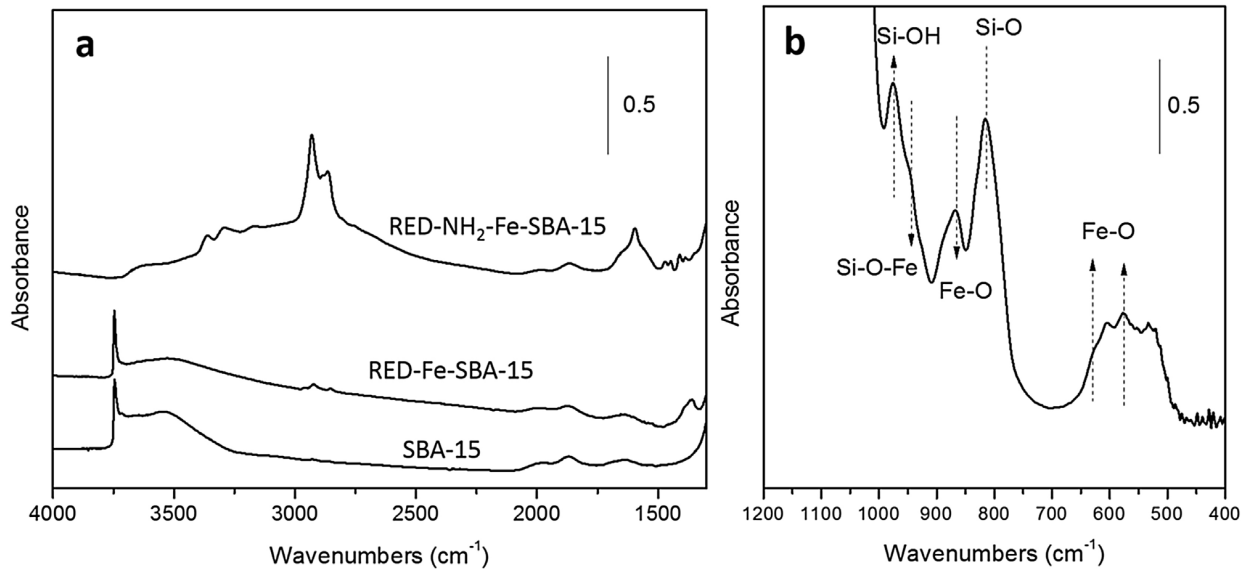
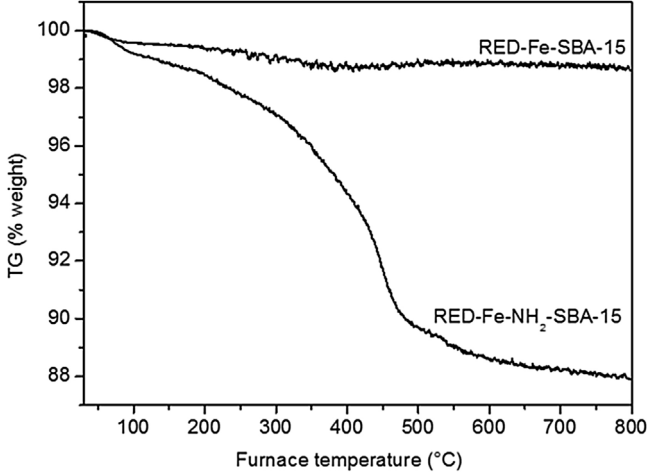Figure 5. TG analysis curves of RED-Fe-SBA-15 and RED-NH$_2$-Fe-SBA-15.

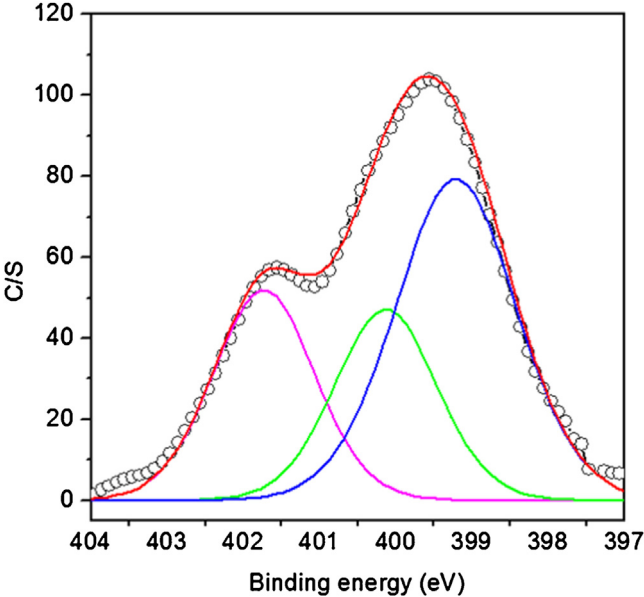Figure 6. XPS spectrum of N 1s for RED-NH$_2$-Fe-SNA-15 sample.

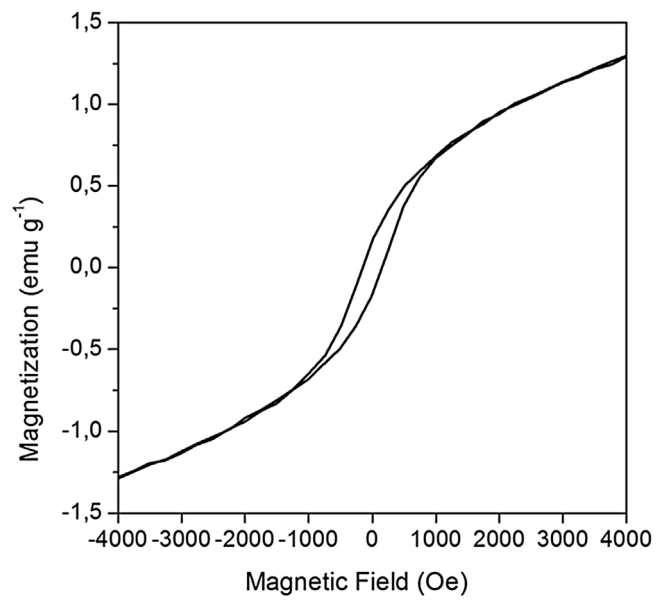Figure 7. Magnetisation curves at 300 K of RED-NH$_2$-Fe-SBA-15 sample.

Figure 8. Removal of glyphosate from tap water by RED-NH$_2$-Fe-SBA-15. Chromatograms of a tap water sample spiked with 2 mg/L glyphosate before (chromatogram A) and after (chromatogram B) the treatment with RED-NH$_2$-FeSBA-15. Recovery of glyphosate from RED-NH$_2$-Fe-SBA-15 using 12.5 mM NaOH solution (chromatogram C). Chromatographic conditions: column: IonPac AG16 (50 mm x 4 mm)(and IonPac AS16 (250 mm x 4 mm); eluent: 35 mM NaOH (1.0 mL/min); detection: suppressed conductivity.